Main-Group Radicals

International Edition: DOI: 10.1002/anie.201504632
German Edition: DOI: 10.1002/ange.201504632

Isolation and Characterization of a Bismuth(II) Radical

*Ryan J. Schwamm, Jeffrey R. Harmer, Matthias Lein, Christopher M. Fitchett, Simon Granville, and Martyn P. Coles**

Abstract: *More than 80 years after Paneth's report of dimethyl bismuth, the first monomeric Bi^{II} radical that is stable in the solid state has been isolated and characterized. Reduction of the diamidobismuth(III) chloride $Bi(NON^{Ar})Cl$ ($NON^{Ar} = [O(SiMe_2NAr)_2]^{2-}$; $Ar = 2,6\text{-}iPr_2C_6H_3$) with magnesium affords the Bi^{II} radical $^{\bullet}Bi(NON^{Ar})$. X-ray crystallographic measurements are consistent with a two-coordinate bismuth in the +2 oxidation state with no short intermolecular contacts, and solid-state SQUID magnetic measurements indicate a paramagnetic compound with a single unpaired electron. EPR and density functional calculations show a metal-centered radical with >90% spin density in a p-type orbital on bismuth.*

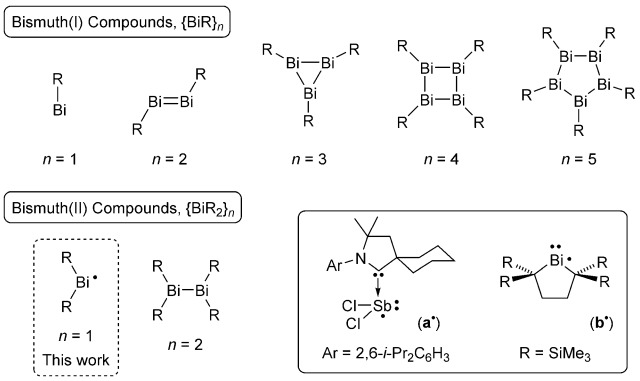

Figure 1. Structural types of reduced bismuth compounds: $\{BiR\}_n$ ($n = 1$–5) and $\{BiR_2\}_n$ ($n = 1$, 2). Inset: Group 15 radicals recently identified in solution.

The first reported example of a Group 15 metalloid in the divalent oxidation state was the cacodyl dimer $Me_2AsAsMe_2$, a compound intimately linked with the origins of organometallic chemistry.[1] Despite this seminal discovery, it was not until 170 years later that Sb^{II}[2] and Bi^{II}[3] compounds were synthesized, reflecting an increased tendency for the heavier elements to undergo disproportionation to M^{III} and M^0. Examples of dibismuthanes $\{BiR_2\}_2$ (R = Me, Et, $SiMe_3$) were first reported in 1982,[4] with a structural report the following year (R = Ph) that confirmed formation of a molecular dimer containing a Bi–Bi single bond.[5] These studies led to a family of reduced diorganobismuth(II) $\{BiR_2\}_n$, ($n = 2$) and monoorganobismuth(I) $\{BiR\}_n$ ($n = 2$–5) compounds (Figure 1).[6] However, with the exception of a unique organobismuth(I) compound,[7] all isolated examples contain homonuclear Bi–Bi bonds, which for divalent Bi^{II} compounds renders the compounds diamagnetic.

The limited number of energetically accessible valence orbitals in main-group elements has led to far fewer examples of stable or persistent metal-centered radicals compared with the transition metals.[8] Notwithstanding this restriction, significant advances continue to be made in Group 15 chemistry, with isolable monomeric phosphorus radicals,[9] and biradicals[10] recently reported. For the heavier elements, an antimony radical has been observed in solution by EPR spectroscopy (**a**•, Figure 1),[11] whereas for bismuth reports remain limited[12] to a tantalizing glimpse of a persistent Bi^{II} radical (**b**•, Figure 1), formed in situ from the dissociation of the corresponding diorganobismuthane.[13] The lack of an observable EPR signal for **b**•, and the inability to characterize **a**• or **b**• in the solid state, demonstrate that neither system is suitable for the isolation of stable radical species.

The novel diamido bismuth(III) chloride, $Bi(NON^{Ar})Cl$ (**1**, $NON^{Ar} = [O(SiMe_2NAr)_2]^{2-}$, Ar = 2,6-diisopropylphenyl)[14] was synthesized in a straightforward metathesis reaction using $Li_2(NON^{Ar})$ and $BiCl_3$. X-ray crystallography showed a monomeric, three-coordinate bismuth supported by κ^2-*N*,*N*′-coordination of the $[NON^{Ar}]$ ligand and a terminal chloride (Supporting Information, Figure S1). Hirshfield surface (HS) analysis[15] indicated that the only intermolecular contacts involving bismuth are weak Bi···H (1.3% of HS) and Bi···π(arene)[16] (1.2% of HS) interactions (Supporting Information, Figure S2, Table S1), with the shortest interaction between Bi···C19′ at a distance of 3.715(4) Å. This contrasts with the molecular structure of $Bi(Me_2Si\{NAr\}_2)Cl$,[17] in which Bi···Cl and Bi···π(arene) interactions generate a trimeric aggregate, leading us to conclude that the $[NON^{Ar}]$ ligand provides effective steric protection of the bismuth center.

Reduction of **1** with excess Mg proceeded with a color change from pale yellow to red over 12–24 h, affording crystalline $^{\bullet}Bi(NON^{Ar})$ (**2**•) as a dark red crystalline solid (yields >80%).[14] If left for extended (ca. 48 h) periods of time before workup, the reaction mixture decolorizes with

[*] R. J. Schwamm, Dr. M. Lein, Dr. M. P. Coles
School of Chemical and Physical Sciences
Victoria University of Wellington
PO Box 600, Wellington 6012 (New Zealand)
E-mail: martyn.coles@vuw.ac.nz
Dr. J. R. Harmer
Centre for Advanced Imaging, University of Queensland
St Lucia, Queensland 4072 (Australia)
Dr. C. M. Fitchett
Department of Chemistry, University of Canterbury
Christchurch 8041 (New Zealand)
Dr. S. Granville
Robinson Research Institute
Victoria University of Wellington
MacDiarmid Institute of Advanced Materials and Nanotechnology,
Lower Hutt 5046 (New Zealand)

Supporting information for this article is available on the WWW under http://dx.doi.org/10.1002/anie.201504632.

concomitant formation of an insoluble black precipitate, which is presumed to be Bi^0. Work-up afforded colorless crystals of $Mg(NON^{Ar})(THF)_2$ (**3**), the product of over-reduction of the bismuth(II) center and ligand transfer to magnesium.[14] The viability of this reaction pathway was verified by independent synthesis of **3** from the reaction of an isolated **2•** and Mg. An X-ray diffraction analysis of **3** showed a molecular Mg^{II} species with the $[NON^{Ar}]^{2-}$ ligand in a tridentate κ^3-*N*,*O*,*N*′-coordination mode at a five-coordinate magnesium center (Supporting Information, Figure S3).

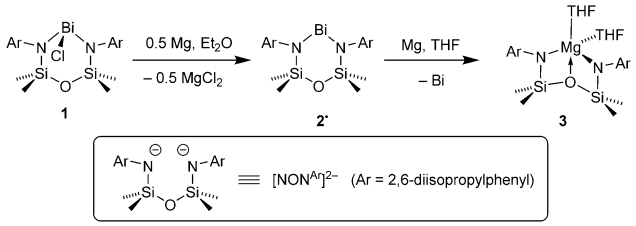

Compound **2•** is a thermally stable, crystalline material with a sharp melting point (range 135–137 °C, decomp. 190 °C). Solid samples stored at room temperature under a dry nitrogen atmosphere retain their color and crystallinity for approximately two weeks. A C_6D_6 solution of **2•** under the same conditions shows the onset of decomposition within 24 h, indicated by gradual decolorizing of the solution and concomitant formation of a solid precipitate; the major diamagnetic species formed in solution during this decomposition was the neutral ligand $(NON^{Ar})H_2$.[18]

The X-ray crystal structure of **2•** confirms a two-coordinate bismuth with retention of a bidentate κ^2-*N*,*N*′-coordination of the diamide (Figure 2).[14] The Bi–N distances of 2.173(4) and 2.172(4) Å are longer than in the Bi^{III} chloride precursor **1** (2.136(2) and 2.149(2) Å) despite the reduced coordination number. The Bi and O atoms are located on a glide plane (Supporting Information, Figure S4), generating chains of molecules parallel to the *b*-axis of the unit cell. HS analysis shows a weak intermolecular Bi···O′ interaction at 3.4476(1) Å, corresponding to 1.4% of the surface area (Supporting Information, Figure S5). Although this distance is within the sum of the van der Waals radii (Σ_{vdW} (Bi,O) = 3.80 Å),[19] it is considerably longer than the sum of the covalent radii (Σ_{cov} (Bi,O) = 2.16 Å), and is comparable to the Bi···O distance of 3.455(2) Å in the charge-separated compound $[BiAr'_2][OAr'']$ (Ar′ = 2,6-$(Me_2NCH_2)_2C_6H_3$, Ar″ = 2,6-$(t\text{Bu})_2C_6H_3$).[20]

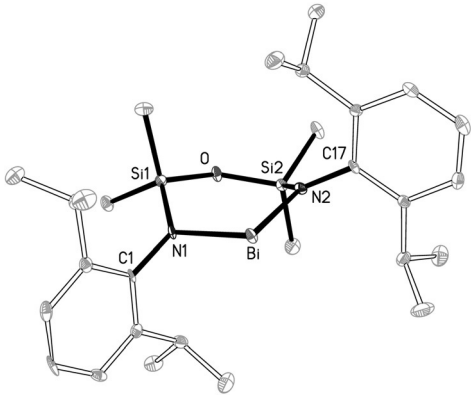

Figure 2. Molecular structure of •Bi(NON^{Ar}), **2•** (ellipsoids set at 30% probability, H-atoms omitted for clarity). Selected bond lengths [Å] and angles [°]: Bi–N1 2.173(4), Bi–N2 2.172(4), Bi···O 3.6687(1), N1–Si1 1.732(5), N2–Si2 1.720(5), Si1–O 1.628(4), Si2–O 1.644(4); N1-Bi-N2 94.70(16), Bi-N1-Si1 123.1(2), Bi-N2-Si2 124.3(2), N1-Si1-O 107.9(2), N2-Si2-O 107.6(2), Si1-O-Si2 138.3(2).

The room-temperature ^{1}H NMR spectrum of **2•** showed broadened and shifted ligand resonances (δ_H +10.75 to −1.56), suggestive of a paramagnetic substance in solution (Supporting Information, Figure S6). The peaks did not sharpen upon cooling the sample to 193 K, which is evidence that aggregation to diamagnetic species containing Bi–Bi bonds was not occurring.[13] The magnetic moment μ_{eff} (293 K) determined by a variation of Evans' method adapted for large, weakly paramagnetic molecules (Supporting Information, Eqs. (S1) and (S2)),[21] was 1.8(±0.1) μ_B, consistent with the presence of a single unpaired electron. These calculations include a diamagnetic correction obtained from the new two-coordinate lead(II) compound, $Pb(NON^{Ar})$ (**4**; Supporting Information, Figure S7).[14]

The room temperature UV/Vis spectrum of **2•** shows absorption bands at λ_{max} 417 and 482 nm (Figure 3), assigned

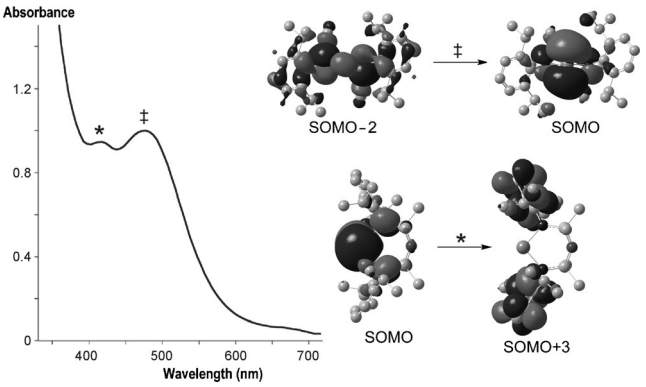

Figure 3. Electronic absorption spectrum of **2•** (1.0 mmol, Et_2O). Transition (*), λ = 417 nm; ε = 946 $mol^{-1}\,dm^3\,cm^{-1}$. Transition (‡), λ = 482 nm, ε = 1000 $mol^{-1}\,dm^3\,cm^{-1}$. Inset: the orbitals associated with the absorptions, from time-dependent density functional theory (TD-DFT).

to electronic transitions involving the singly occupied molecular orbital (SOMO; Supporting Information, Figure S9), as determined by TD-DFT (Figure S8, Tables S2–S4). The more intense absorption at 482 nm involves a predominantly n(N)→6p(Bi) ligand-to-metal transfer whilst the weaker absorption at 417 nm involves a metal-to-ligand transfer from the SOMO to the aromatic system of nitrogen substituents (6p(Bi)→π(C–C)). For radical **b•** (Figure 1), a single absorption band at 543 nm was assigned to the n(Bi)→6p(Bi) transition.[13]

The paramagnetism of **2•** was unambiguously confirmed by EPR spectroscopy.[14] X- and Q-band field-sweep EPR

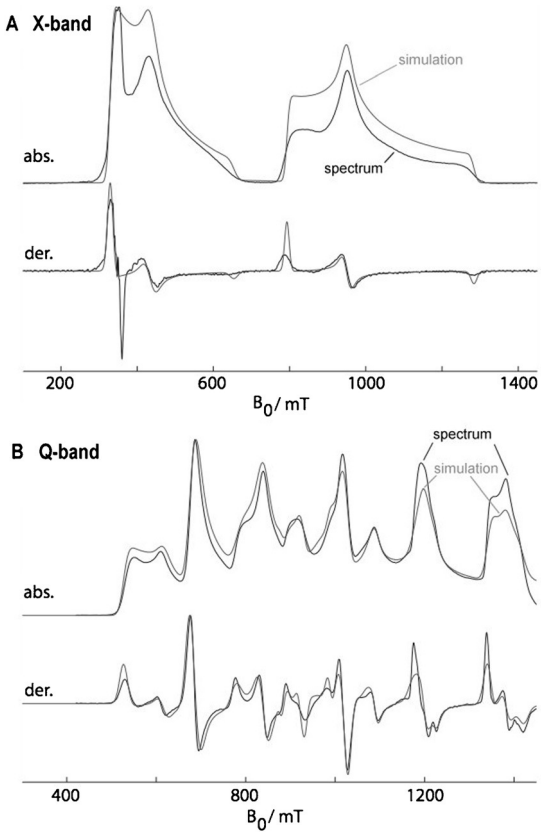

Figure 4. Field-sweep EPR spectra for **2**$^{\bullet}$ measured in frozen 1:1 hexane/toluene solution (black), with the corresponding simulations (gray). A) X-band (9.7462 GHz) echo-detected EPR spectrum; B) Q-band (34.2113 GHz) FID-detected EPR spectrum. The first-derivative spectra (der.) are calculated numerically from the absorption (abs.) spectra. The principal *g*-values and metal hyperfine couplings *A* are (corresponding DFT values are italicized and in parentheses): g_1, g_2, $g_3 = 1.621$, 1.676, 1.832 (*1.714, 1.944, 2.025*); $A(^{209}\text{Bi}) = -2804$, -3830, $-4764 = -3799 + (995, -31, -965)$ MHz, $(-6090 + (1613, -801, -812)$ MHz. The negative sign of the experimental hyperfine couplings were assigned to give positive spin population.

spectra are shown in Figure 4, along with corresponding simulations (Supporting Information, Table S5) computed from a spin Hamiltonian model including a *g*-matrix with principle values $(g_1, g_2, g_3) = (1.676, 1.832, 1.621)$ and a bismuth hyperfine interaction $A(^{209}\text{Bi}) = (-2804, -3830, -4764)$ MHz (^{209}Bi, 100% abundant, $I = 9/2$). The large *g*-value anisotropy and Bi hyperfine couplings demonstrate unequivocally that the radical is metal centered. At both X-band and Q-band, signals are observed over nearly the full sweep range of the magnet, 0–1.5 T. The characteristics of the spectra are interpreted with reference to the energy level diagram computed along the g_1 axis (Supporting Information, Figure S10). As a result of the large Bi hyperfine couplings, only two of the ten EPR transitions can be excited at X-band (for $I = 9/2$ there are $2I + 1 = 10$ allowed EPR transitions at high field), which correspond to the two separated regions of signal intensity in the EPR spectrum of Figure 4A. The spectral width of these two features is a combination of the *g*-value and large Bi hyperfine anisotropy. The higher energy microwave quanta of the Q band is able to excite all ten EPR transitions, but only the lowest six are represented in Figure 4B, up to the maximum field of 1.5 T. The spectrum shape, as for the X-band spectrum, is a complicated combination of the *g*-value and hyperfine anisotropy.

An experimental estimate of the bismuth spin population, ρ(Bi), can be made by splitting the hyperfine couplings into isotropic $a_{iso} = -3799$ MHz and anisotropic $A_T = (995, -31, -964)$ MHz contributions (with a mean $T = (-31–964)/2 = -498$ MHz) and scaling with tabulated Bi hyperfine couplings for s ($-66\,195$ MHz) and p (-567 MHz) atomic orbitals, respectively:[22] $\rho \approx (-3799/-66\,195) + (-498/-567) = 0.94$. This estimate uses the average values for the anisotropic hyperfine coupling parameter *T* as the Bi hyperfine coupling is rhombic. The DFT computed *g*- and hyperfine values are listed in Figure 4 and are in reasonable agreement with the experimental values. The DFT model features $\rho^{DFT}(\text{Bi}) = 0.92$.

The extent of spin population delocalization over the ligands was characterized using the high-resolution pulse technique, hyperfine sublevel correlation spectroscopy (HYSCORE),[23] to measure couplings not resolved in the field-sweep EPR spectra. Q-band HYSCORE data revealed small ^{14}N and ^{29}Si hyperfine couplings (Supporting Information, Figure S11). The ^{14}N hyperfine couplings, circa 15–21 MHz, estimated from the spectra amounts to a small $\rho(\text{N}) < 0.05$ on each nitrogen. Similarly the very small ^{29}Si hyperfine coupling of about -2 to $+4$ MHz amount to $\rho(\text{Si}) < 0.01$. These experimental values support the DFT model of electronic structure where $A^{DFT}(^{14}\text{N}) = (-1.7, -2.7, 12.0)$ MHz, $\rho^{DFT}(\text{N}) = 0.024$ and $A^{DFT}(^{29}\text{Si}) = (1.4, 2.1, 2.7)$ MHz, $\rho^{DFT}(\text{Si}) = 0.007$.

The magnetization of **2**$^{\bullet}$ as a function of field (M–H) at 2 K (Supporting Information, Figure S12A) and as a function of temperature (M–T) in a field of 100 Oe (Supporting Information, Figure S12B) show the characteristics of paramagnetism.[14] The M–H data is fit well by the Brillouin function for paramagnetic ions (Supporting Information, Eqs. (S3) and (S4)),[24] using an average of the three *g*-factor values determined by EPR spectroscopy ($g_{ave} = 1.79053$) and net angular momentum $J = 0.5$, corresponding to a single unpaired electron per $^{\bullet}$Bi(NON^{Ar}) unit. The number of paramagnetic ions, determined from fits to M–H data taken at 2 and 10 K, is $N = 8.2 \pm 1.0 \times 10^{17}$, which indicates all of the $^{\bullet}$Bi(NON^{Ar}) units in the sample have unpaired electrons that contribute to the magnetism. The M–T data fit Curie's law (Supporting Information, Eq. (S5)) with a μ_{eff} of $1.46 \pm 0.03\ \mu_B$, close to the value for a $J = 0.5$ paramagnetic ion of μ_{eff} of 1.73 μ_B.[25] These data support the EPR measurements, confirming that **2**$^{\bullet}$ is paramagnetic resulting from a single unpaired electron per unit.

Although the possibility exists that **2**$^{\bullet}$ is the Bi^{III} hydride Bi(NON^{Ar})(H),[26] we rule this out based on the following data: 1) the demonstrable paramagnetic character of **2**$^{\bullet}$ in the solution and solid states; 2) the isomorphous X-ray diffraction data for **2**$^{\bullet}$ and the lead(II) analogue **4** (monoclinic, $P2_1/c$; Supporting Information, Figure S8); 3) the increased Bi–N bond lengths compared with **1** and the lack of any regions of residual electron density in a sensible position for a trigonal pyramidal bismuth hydride.[26a] Further evidence derives from

the attempted synthesis of the Bi^{III} hydride from the reaction of **1** with lithium triethylborohydride in a sealed NMR tube at room temperature. Analysis of the reaction mixture by ^1H NMR spectroscopy showed the presence of H_2 (singlet at δ_H 4.47 in C_6D_6) and formation of the radical **2**$^{\bullet}$, suggesting instability of the postulated hydride; this pathway has previously been used to synthesize dibismuthanes R_2BiBiR_2 ($R = CH(SiMe_3)_2$, mesityl).[26b,27]

Keywords: bismuth · EPR · main-group elements · paramagnetism · stable radicals

How to cite: *Angew. Chem. Int. Ed.* **2015**, *54*, 10630–10633
Angew. Chem. **2015**, *127*, 10776–10779

[1] D. Seyferth, *Organometallics* **2001**, *20*, 1488–1498.
[2] F. A. Paneth, *Trans. Faraday Soc.* **1934**, *30*, 179–181.
[3] F. A. Paneth, H. Loleit, *J. Chem. Soc.* **1935**, 366–371.
[4] a) A. J. Ashe III, E. G. Ludwig, *Organometallics* **1982**, *1*, 1408–1408; b) H. J. Breunig, D. Müller, *Angew. Chem. Int. Ed. Engl.* **1982**, *21*, 439–440; *Angew. Chem.* **1982**, *94*, 448–448; c) G. Becker, M. Rößler, *Z. Naturforsch. B* **1982**, *37*, 91–96.
[5] F. Calderazzo, A. Morvillo, G. Pelizzi, R. Poli, *J. Chem. Soc. Chem. Commun.* **1983**, 507–508.
[6] a) H. J. Breunig, *Z. Anorg. Allg. Chem.* **2005**, *631*, 621–631; b) G. He, O. Shynkaruk, M. W. Lui, E. Rivard, *Chem. Rev.* **2014**, *114*, 7815–7880.
[7] P. Šimon, F. de Proft, R. Jambor, A. Růžička, L. Dostál, *Angew. Chem. Int. Ed.* **2010**, *49*, 5468–5471; *Angew. Chem.* **2010**, *122*, 5600–5603.
[8] P. P. Power, *Chem. Rev.* **2003**, *103*, 789–810.
[9] a) P. Agarwal, N. A. Piro, K. Meyer, P. Müller, C. C. Cummins, *Angew. Chem. Int. Ed.* **2007**, *46*, 3111–3114; *Angew. Chem.* **2007**, *119*, 3171–3174; b) S. Roy, A. C. Stückl, S. Demeshko, B. Dittrich, J. Meyer, B. Maity, D. Koley, B. Schwederski, W. Kaim, H. W. Roesky, *J. Am. Chem. Soc.* **2015**, *137*, 4670–4673; c) F. Hirakawa, H. Ichikawa, S. Ishida, T. Iwamoto, *Organometallics* **2015**, *34*, 2714–2716.
[10] A. Hinz, A. Schulz, A. Villinger, *Angew. Chem. Int. Ed.* **2015**, *54*, 2776–2779; *Angew. Chem.* **2015**, *127*, 2815–2819.
[11] R. Kretschmer, D. A. Ruiz, C. E. Moore, A. L. Rheingold, G. Bertrand, *Angew. Chem. Int. Ed.* **2014**, *53*, 8176–8179; *Angew. Chem.* **2014**, *126*, 8315–8318.
[12] T. Sasamori, E. Mieda, N. Nagahora, K. Sato, D. Shiomi, T. Takui, Y. Hosoi, Y. Furukawa, N. Takagi, S. Nagase, N. Tokitoh, *J. Am. Chem. Soc.* **2006**, *128*, 12582–12588.
[13] S. Ishida, F. Hirakawa, K. Furukawa, K. Yoza, T. Iwamoto, *Angew. Chem. Int. Ed.* **2014**, *53*, 11172–11176; *Angew. Chem.* **2014**, *126*, 11354–11358.
[14] Full experimental details, characterization, and details of computational experiments can be found in the Supporting Information. CCDC 1056183 (**1**), 1056184 (**2**$^{\bullet}$), 1056185 (**3**), and 1056186 (**4**) contain the supplementary crystallographic data for this paper. These data can be obtained free of charge from The Cambridge Crystallographic Data Centre.
[15] M. A. Spackman, D. Jayatilaka, *CrystEngComm* **2009**, *11*, 19–32.
[16] I. Caracelli, I. Haiduc, J. Zukerman-Schpector, E. R. T. Tiekink, *Coord. Chem. Rev.* **2013**, *257*, 2863–2879.
[17] B. M. Day, M. P. Coles, *Organometallics* **2013**, *32*, 4270–4278.
[18] D. B. Leznoff, G. Mund, K. C. Jantunen, P. H. Bhatia, A. J. Gabert, R. J. Batchelor, *J. Nucl. Sci. Technol.* **2002**, *39*, 406–409.
[19] J. Emsley, *Die Elemente*, Walter de Gruyter, Berlin, **1994**.
[20] I. J. Casely, J. W. Ziller, B. J. Mincher, W. J. Evans, *Inorg. Chem.* **2011**, *50*, 1513–1520.
[21] C. Piguet, *J. Chem. Educ.* **1997**, *74*, 815.
[22] J. R. Morton, K. F. Preston, *J. Magn. Reson.* **1978**, *30*, 577–582.
[23] a) A. Schweiger, G. Jeschke, *Principles of Pulse Electron Paramagnetic Resonance*, Oxford University Press, Oxford, **2001**; b) P. Höfer, A. Grupp, H. Nebenführ, M. Mehring, *Chem. Phys. Lett.* **1986**, *132*, 279–282.
[24] N. W. Ashcroft, N. D. Mermin, *Solid State Physics*, Saunders College Publishing, New York, **1976**.
[25] M. McElfresh, Fundamentals of Magnetism and Magnetic Measurements Featuring Qunatum Design's Magnetic Property Measurement System, Quantum Design, Purdue University, **1994**.
[26] a) N. J. Hardman, B. Twamley, P. P. Power, *Angew. Chem. Int. Ed.* **2000**, *39*, 2771–2773; *Angew. Chem.* **2000**, *112*, 2884–2886; b) G. Balázs, H. J. Breunig, E. Lork, *Organometallics* **2002**, *21*, 2584–2586.
[27] L. Balázs, H. J. Breunig, E. Lork, *Z. Naturforsch. B* **2005**, *60*, 180–182.

Received: May 21, 2015
Published online: July 27, 2015

